Carbohydrate Polymers 76 (2009) 232–238

Contents lists available at ScienceDirect

Carbohydrate Polymers

journal homepage: www.elsevier.com/locate/carbpol

Preparation and properties of chitosan/carbon nanotube nanocomposites using poly(styrene sulfonic acid)-modified CNTs

Ying-Ling Liu *, Wei-Hong Chen, Yu-Hsun Chang

R&D Center for Membrane Technology and Department of Chemical Engineering, Chung Yuan Christian University, #200, Chung-Pei Road, Chungli, Taoyuan 32023, Taiwan

ARTICLE INFO

Article history:
Received 19 August 2008
Received in revised form 15 October 2008
Accepted 17 October 2008
Available online 5 November 2008

Keywords:
Chitosan
Carbon nanotube
Nanocomposite

ABSTRACT

Poly(styrene sulfonic acid)-functionalized carbon nanotubes (CNT-PSSA), which was obtained with atom transfer radical polymerization (ATRP), was utilized in preparation of chitosan/CNT nanocomposites (CH/CNT-PSSA). Chemical linkages between chitosan and CNTs form in the nanocomposites through the reaction between the sulfuric acid groups of CNT-PSSA and the amino groups of chitosan, to warrant the homogenous dispersion of CNTs. The CH/CNT-PSSA nanocomposites were superior to the neat chitosan polymer in thermal and mechanical properties, water and solvent uptakes, bond water ratios, and electrical conductivity. The attractive property of the CH/CNT-PSSA nanocomposites also implied their application potentials for separation membranes and sensor electrodes.

1. Introduction

Chitosan is a nature polysaccharide bearing amino and hydroxyl groups showing wide application potentials in biology, medicine, food, electrochemistry, and membrane separation due to its attractive characteristics of low price, biocompatibility, hydrophilicity, moderate mechanical property, and chemical versatility. Modifications on chitosan were widely studied to improve the solubility of chitosan in water and consequently to improve its processing properties (Hirano, Yamaguchi, & Kamiya, 2003; Lu, Song, Cao, Chen, & Yao, 2004; Sashiwa, Yamamori, Ichinose, Sunamoto, & Aiba, 2003; Sashiwa et al., 2002). On the other hand, preparation of organic/inorganic chitosan nanocomposites also received considerable research interests (Darder, Colilla, & Ruiz-Hitzky, 2003; Darder et al., 2006; Gutierrez, Jobbagy, Ferrer, & del Monte, 2008; Hu, Chan, & Szeto, 2008; Lin et al., 2005; Podsiadlo, Tang, Shim, & Kotov, 2007; Wang, Chen, & Tong, 2006; Wang, Du, Yang, Tang, & Luo, 2008; Wang & Wang, 2007; Xu, Ren, & Hanna, 2006; Zhang, Wang, & Wang, 2007). Chitosan, possessing amine groups, could be utilized as an agent for clay intercalation (Darder et al., 2003). Preparation and property of chitosan/clay nanocomposites were also studied (Darder et al., 2003; Darder et al., 2006; Lin et al., 2005; Podsiadlo et al., 2007; Wang & Wang, 2007; Wang et al., 2006; Wang et al., 2008; Xu et al., 2006; Zhang et al., 2007). Some potential applications of the chitosan/clay nanocomposites were bulk-modified electrodes (Darder et al., 2003) and antimicrobial materials (Wang et al., 2008). Besides, layer-by-layer chitosan/montmorillonite nanocomposites were also reported to exhibit a counterintuitive effect of molecular strength on the macroscale mechanical properties of nanocomposites (Podsiadlo et al., 2007). On the other hand, some papers reported the preparation of chitosan-gold nanocomposites and their applications for biosensors (Santos, Goulet, Pieczonka, Oliveira, & &Aroca, 2004) and cell culture (Ding, Hao, Xue, & Ju, 2007). Our previous work also reported the chitosan/silica nanocomposites and their uses in membrane dehydration on ethanol/water mixtures (Liu, Hsu, Su, & Lai, 2005a).

Beside clay and silica nanoparticles, carbon nanotube (CNT) is another promising nano-filler for preparation of polymer nanocomposites (Dong, Wang, He, & Li, 2008; Jeon, Tan, & Baek, 2008; Jin, Yoon, Park, & Bang, 2008; Wang, Dai, & Yarlagadda, 2005a; Xu, Wang, & Douglas, 2008). Chitosan and CNTs were reasonably integrated to form chitosan/CNT nanocomposites (Hao, Ding, Zhang, & Ju, 2007; Kandimalla & Ju, 2006; Ke et al., 2007; Lu, Jiang, Song, Liu, & Jiang, 2005; Qiu, Guo, Liang, & Xiong, 2007; Wang, Shen, Zhang, & Tong, 2005b; Xu, Gao, Chen, & Dong, 2005). It is noteworthy that performance and properties of nanocomposites are highly affected with the interfacial compatibility between the polymer and the nanofillers. Improvement on the compatibility between chitosan and CNTs is therefore very critical in chitosan/CNT nanocomposite preparation. One approach was uses of acid-treated CNTs, which formed hydrogen-bonds with chitosan chains to improve the interfacial compatibility between chitosan and CNTs (Wang et al., 2005b). Although the chitosan/CNT nanocomposites showed higher tensile modulus and mechanical strengths than did neat chitosan, the loading amounts of CNT were not high. Chitosan/CNT nanocomposite was also prepared through the layer-by-layer assembly of chitosan and acid-treated CNT (Xu et al., 2005). To further increase the interaction strength between chitosan and CNT, covalent linkages were introduced to the chito-

* Corresponding author. Tel.: +886 3 2654130; fax: +886 3 2654199.
E-mail address: ylliu@cycu.edu.tw (Y.-L. Liu).

0144-8617/$ - see front matter © 2008 Elsevier Ltd. All rights reserved.
doi:10.1016/j.carbpol.2008.10.021

san/CNT interfaces. Acyl chloride-modified CNT was utilized with Ke et al. (2007) to prepare chitosan-covered CNT, in which covalent linkages formed through the reaction between the amino groups of chitosan and the acyl chloride groups of the modified CNTs. This approach still employed the step of CNT acid-treatment, which was somewhat dangerous and brought bundle cut to CNTs. Therefore, in this work we reported another facile approach to prepare chitosan/CNT nanocomposites using poly(styrene sulfonic acid) (PSSA)-functionalized CNTs (CNT-PSSA). The sulfonic acid groups of PSSA provide chemical reactivity and interfacial compatibility between CNT-PSSA and chitosan. Moreover, the PSSA-modified CNTs were readily soluble in acidic aqueous solution of chitosan, to warrant the well dispersion of CNT-PSSA in chitosan. In addition to physical and mechanical properties, the electric conductivities of the prepared chitosan/CNT nanocomposites were also examined to probe their potential applications in electrodes and sensors. On the other hand, the chitosan/CNT nanocomposites were also used as selective separation membranes. The dehydration performance of the nanocomposite membranes on ethanol aqueous solutions was examined to probe their applications in purification of biomass.

2. Experimental

2.1. Materials

Multi-walled carbon nanotube (MWNT) was received from the CNT Co., Ltd., Incheon, Korea. Commercial products of sodium 4-styrenesulfonate (NaSS, Fluka Chemie), 1-bromoethylbenzene (BEB, Tokyo Chem. Ind., purity > 95%), 1,1,4,7,7-pentamethyldiethylenetriamine (PMDETA, Aldrich, 99% in purity), copper(I) bromide (CuBr, Aldrich, 99.999% in purity), and chitosan with a degree of deacetylation of 85% (Sigma Chemical Co.) were used as received. *N*,*N*-dimethylformamide (DMF) was purchased from TEDIA Chem. Co., and dried over molecular sieve before use.

2.2. Characterization

FTIR-ATR spectra were obtained with a Perkin-Elmer Spectrum One FTIR equipped with a multiple internal reflectance apparatus and a ZnSe prism as an internal reflection element. X-ray photoelectron spectroscopy (XPS) analysis was conducted with a VG MICROTECH MT-500 ESCA (British) using a Mg K_α line as a radiation source. The background pressure in the analytical chamber was 1.0×10^{-5} Pa. Raman spectra were obtained using a Renishaw InVia Raman spectrometer employing a He–Ne laser of 1 mW radiating on the sample operating at 632.8 nm. The molecular weights of polymers were measured with a gel permeation chromatography (GPC) composed of a LAB-Alliance Series III pump, an RI 2000 refractive index detector, and a PLgel Mixed D column with poly(styrene) gel particles of 5 μm in diameter as stationary phase. The elution was performed with DMF in a flow rate of 1.0 ml/min at 40 °C. Mono-dispersed styrene samples were used as standards for molecular weight calibration. Thermogravimetric analysis (TGA) was performed with an instrument from Thermal Analysis Incorporation (TA-TGA 2050) at a heating rate of 10 °C/min under nitrogen atmosphere. Differential scanning calorimetry (DSC) was performed with a TA-DSC Q100 at a heating rate of 10 °C/min. Water contact angles were measured with an angle-meter (Automatic Contact Angle Meter, Model CA-VP, Kyowa Interface Science Co., Ltd. Japan) at room temperature. Distilled water (5 μL) was dropped on the sample surface at ten different sites. The average of ten measured values for a sample was taken as its water contact angle. Scanning electron micrographs (SEM) were obtained with a Hitachi S-4800 field-emission SEM. High-resolution transmission electron microscopy (HRTEM) was conducted with a JEOL JEM-2010 HRTEM. Mechanical property of materials was analyzed with an Instron 5543 analyzer at an elongation rate of 0.5 mm/min. Electrical conductivity was measured with a Solartron 1296A Dielectric Interface equipped with a Solartron 1255B Frequency Response Analyzer at a frequency range of 0.1–1 MHz.

2.3. Pervaporation operation

Pervaporation dehydration operation was conducted with a conventional process (Liu et al., 2005a). The effective area of the membrane was 9.8 cm^2. The temperature of the feeding solution was 70 °C and the downstream (permeate side) pressure was 667–1067 Pa. While the system was in steady-state (usually after a pre-operation in 2 h), the data was taken in 1 h period of continuing operation. The compositions of feeding solutions and permeates were determined with a gas chromatography (China Chromatography GC-8700 T). The separation factor ($SF_{water/organic\ compound}$) was calculated from equation of

$$SF_{water/organic\ compound} = (Y_{water}/Y_{organic\ compound})/(X_{water}/X_{organic\ compound}),$$

where Y and X are the concentrations of permeate and feeding solutions, respectively, and the subscription (water and organic compound) indicates the species. Permeation flux was determined by measuring the weight of permeate liquid through the membrane at given time. Data was obtained from the average of measuring results from four pieces of separate membranes.

2.4. Preparation of poly(sodium styrene sulfonate) (PNaSS)

Poly(sodium styrene sulfonate) (PNaSS) was prepared from atom transfer radical polymerization (ATRP) of NaSS. NaSS (4.12 g, 20 mmol), CuBr (28.7 mg, 0.2 mmol), and PMDETA (34.6 mg, 0.6 mmol) were dissolved in 30 mL of DMF and the solution was charged in a 50 mL round-bottom flask. After purging with dry argon for 15 min, BEB (37 mg, 0.2 mmol) was added into the reaction system. The reaction system was de-gassed for 3 times and then reacted at 130 °C for 30 h. The reaction mixture was diluted with DMF (20 mL). PNaSS was obtained with precipitation from excess acetone and purified by repeated dissolution–precipitation process for 3 time. The product yield is 72%. The number-average molecular weight (M_n) and the polydispersity index (PDI) of PNaSS measured with GPC are 9,800 g/mol and 1.2, respectively.

2.5. Preparation of poly(styrene sulfonic acid) (PSSA)-functionalized CNTs (CNT-PSSA)

MWNT (0.3 g), CuBr (0.2 mmol, 0.03 g), PMDETA (0.35 mmol, 0.06 g) and 8 mL DMF were charged into a 20 mL reactor. After purging with dry argon for 15 min, PNaSS (1.0 g) was added into the reaction system. The reaction system was de-gassed for 3 times and then reacted at 130 °C for 30 h. The reaction mixture was poured into excess DMF. CNTs were collected with filtration, washed with DMF and hot water for several times in an ultrasonic bath to remove the physically adsorbed compounds, and then dried under vacuum to give the product of CNT-PNaSS (0.24 g). CNT-PNaSS was dispersed in 1 M hydrochloride aqueous solution for 3 h. CNTs were collected with filtration, washed with distilled water, dried under vacuum to give the product of CNT-PSSA (0.22 g).

2.6. Preparation of chitosan/CNT nanocomposites CH/CNT-PSSA

Chitosan (3.0 g) was dissolved in 100 mL 2 wt% acetic aqueous solution. The chitosan solutions were stand overnight. Various amounts of CNT-PSSA were added to the chitosan solutions under

stirring, respectively. CH/CNT-PSSA nanocomposite films were obtained from solution casting and dried under vacuum at 40 °C overnight.

3. Results and discussion

Comparing to surface-functionalized CNTs with short chemical groups, polymer modified CNTs are much attractive to provide better solubility in solvents, higher compatibility with polymers, and more reactive sites for further modifications. Therefore, PSSA chains, which possess sulfonic acid groups, were incorporated to CNT surfaces in this work according to the method reported in our previous work (Liu & Chen, 2007) (Scheme 1). Under the reaction condition of ATRP, addition of PNaSS chains to CNT surfaces is performed by the reaction between the radicals of PNaSS chain ends and the un-saturate sites of CNT surfaces. Treatment of CNT-PNaSS with a dilute hydrochloride aqueous solution converted the sodium sulfonate groups of PNaSS to sulfonic acid groups to result in the poly(styrene sulfonic acid)-functionalized CNTs (CNT-PSSA). The physically absorbed PNaSS chains on CNT surfaces were removed out by washing with solvent and water in an ultrasonic bath. On the other hand, a CNT sample collected from the DMF solution of CNT and PNaSS, in which PNaSS chains were not covalently-linked to CNT, was treated with the same procedure. No organic portions were found with the washed CNT sample. This complemental test confirms the complete removal of non-covalently bonded polymer chains from CNT-PNaSS. The spectra characterizations on the polymer-functionalized CNTs were performed with FTIR, XPS, and Raman (Fig. 1). The organic PSSA chains of CNT-PSSA hybrid was observed in its FTIR spectrum with the absorption peaks at 1653 (phenyl groups), 1411 (asymmetric –SO_2–), and 1173 (symmetric –SO_2–) cm^{-1}. XPS analysis results demonstrated the presence of PNaSS chains in CNT-PNaSS with the signals of $Na_{(1s)}$ at 1072 eV and $O_{(1s)}$ at 530 eV. The appearance of $Br_{(3d)}$ signal at 78 eV in the spectrum also indicates the occurrence of bromine atom transfer to CNTs in the ATRP modification reaction and the success of covalently bonding PNaSS chains to CNT surfaces (Liu & Chen, 2007). The bromine transfer reaction also results in structure changes on CNT, which were examined with Raman spectroscopic analysis (exciting at 633 nm). Pristine CNT exhibited two significant signals at 1315 and 1590 cm^{-1}, representing the disorder sp^3 mode (D band) and the tangential mode (G band) of CNT, respectively. The ratio of D band over G band (D/G ratio) for the pristine CNT was about 0.998. After PNaSS functionalization, some sp^2 hybridized carbons in CNTs converted to be in sp^3 hybridization. Therefore, the D/G ratio of CNT-PSSA increased to 1.78. This change in D/G ratio indicates the success of bonding PNaSS to CNT side walls. Fig. 1-d shows the HRTEM micrograph of CNT-PSSA. The PSSA chains with a layer thickness of about 2 nm could be seen covering on CNT surface. The weight ratio of PSSA chains in CNT-PSSA is about 46 wt%, which was determined with a TGA.

CNT-PSSA is readily soluble in acetic acid aqueous solution of chitosan (CH). Various amounts of CNT-PSSA were added to chitosan solutions. The well-dispersed solutions were then cast into CH/CNT-PSSA-X films, where X denotes the weight percents of CNT-PSSA in the CH/CNT-PSSA-X nanocomposites. The nanocomposite films are transparent. No CNT aggregations existed in the CH/CNT-PSSA nanocomposite films, as shown with their cross-sectional SEM micrographs (Fig. 2). The effect of CNT-PSSA on the thermal stability and degradation behavior of chitosan was studied with TGA (Figure not shown). Pristine chitosan and its nanocomposite exhibited similar thermal stability with temperatures at 5% weight loss (T_{d5}) of about 225 °C. The thermal degradation patterns of CH/CNT-PSSA nanocomposites are also similar to that observed with neat chitosan. Addition of CNT-PSSA to chitosan slightly increased the char yields at 800 °C, due to the presence of non-degradable CNTs. On the other hand, the presence of CNT-PSSA in chitosan matrix enhanced the mechanical properties (Wang et al., 2005b), as shown in Fig. 3. For comparison, a

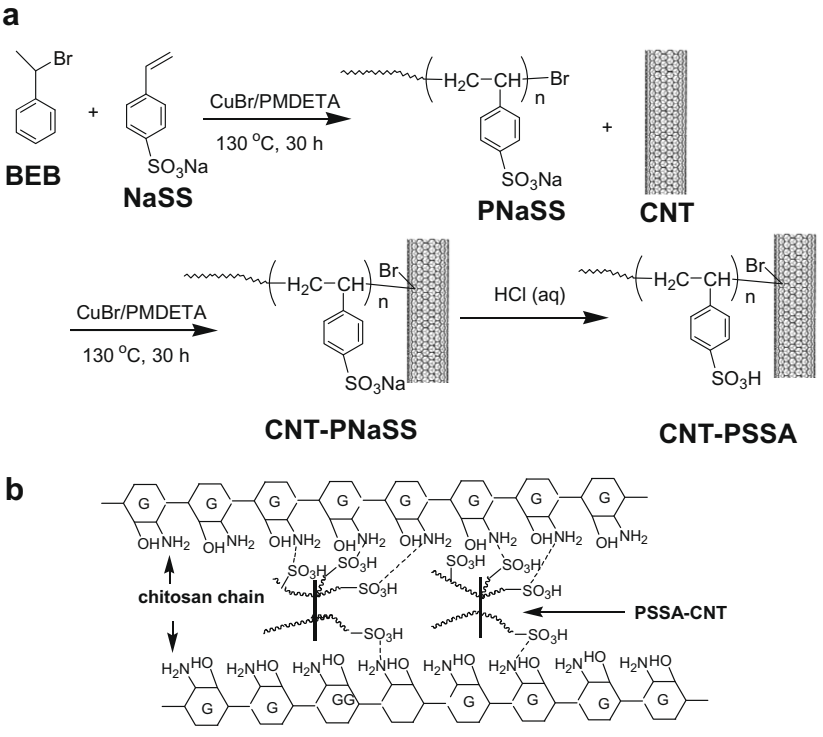

Scheme 1. (a) Preparation of poly(styrene sulfonic acid)-functionalized carbon nanotube (PSSA-CNT); (b) a model representing the linkages between PSSA-CNT and chitosan in chitosan/PSSA-CNT nanocomposites.

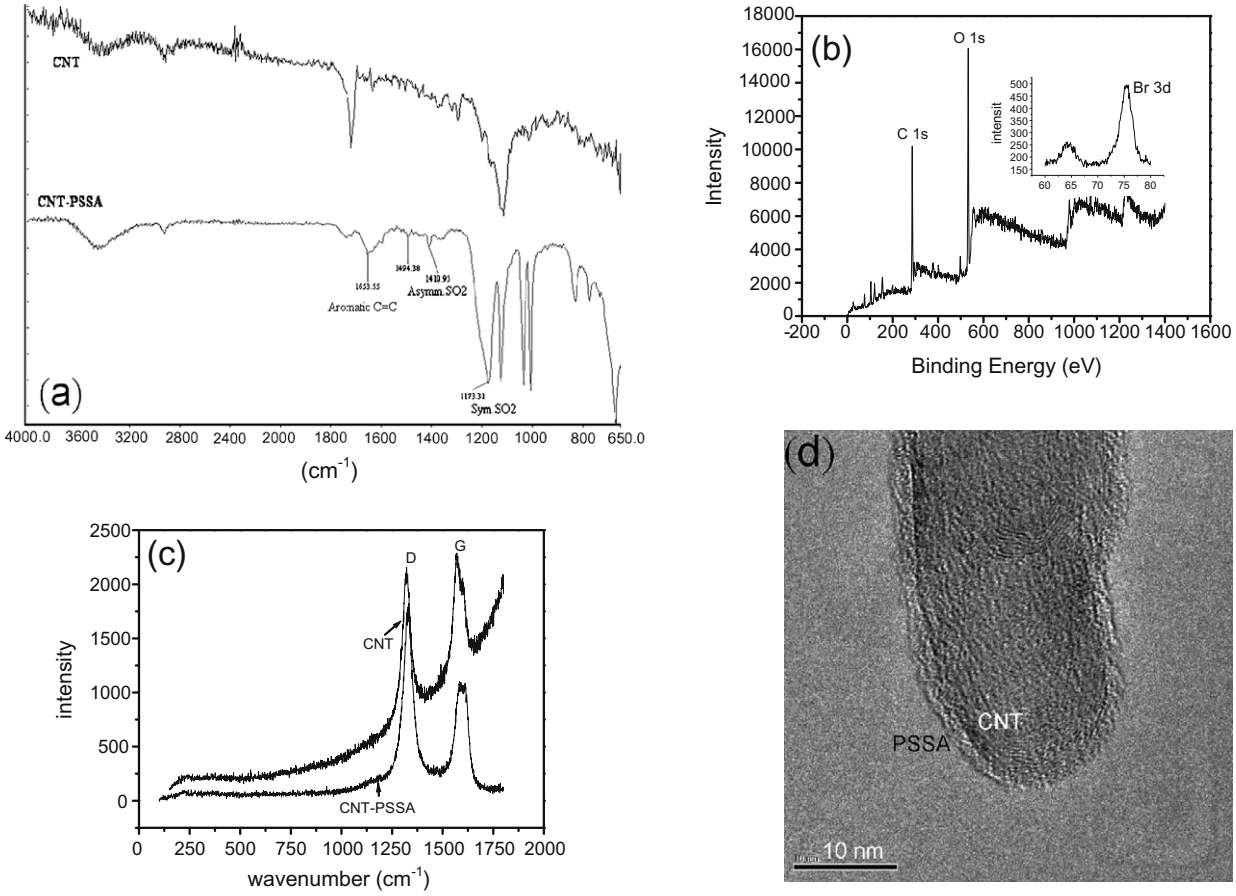

Fig. 1. Characterization on the surface-functionalized CNT-PSSA with (a) FTIR-ATR, (b) XPS, (c) Raman spectrometry, and (d) HRTEM micrograph.

composite possessing 0.5 wt% un-modified CNT (CH/CNT-0.5) was also prepared and analyzed. Neat chitosan showed a tensile strength of 11.6 MPa and a Young's modulus of 580 MPa. The tensile strength and Young's modulus of CH/CNT-PSSA-1.5 are 30.4 MPa and 2815 MPa, respectively. Both tensile strengths and Young's modulus of the CH/CNT-PSSA nanocomposites are greater than those of chitosan and increase with increasing the CNT-PSSA amounts in the nanocomposites. Moreover, formation of nanocomposites with CNT-PSSA also increased the elongation at break of chitosan from 2.0% to 6.1%. Small amount of water absorbed in the nanocomposite films might contribute to the elongation increase. The water-maintaining ability of the CH/CNT-PSSA nanocomposites would be discussed later. On the other hand, it is noticeable that the tensile strength and Young's modulus of CH/CNT-0.5 are of about 67% and 87%, respectively, comparing to the corresponding values of CH/CNT-PSSA-0.5. It is demonstrated that the presence of PSSA chains on CNT surfaces improves the interfacial compatibility between chitosan and CNTs. Due to not possessing PSSA chains and relatively poor less water-maintaining ability, CH/CNT-0.5 breaks at an elongation of about 2.0%, which is similar to the elongation of neat chitosan and is smaller than that of CH/CNT-PSSA-0.5.

The water contact angle measured with CH/CNT-PSSA-1.5 is 86°. All other CH/CNT-PSSA nanocomposites show water contact angles of about 72–74°, which are similar to the value measured with neat chitosan (73°). The presence of PSSA chains, although they are relatively hydrophilic, might induce the chitosan chain rotation pulling the hydrophilic amino and hydroxyl groups of chitosan toward the inner of nanocomposite films by means of the interaction between PSSA and chitosan. The surface hydrophilicity of CH/CNT-PSSA-1.5 is thus reduced. Addition of CNT-PSSA also depresses the water uptakes of chitosan films (Fig. 4). However, the depression amplitude is not as significant comparing to the chitosan films modified with sulfonated silica nanoparticles (Liu & Chen, 2007), because of the small amounts of CNTs loaded in CH/CNT-PSSA nanocomposites. The uptake values of the nanocomposite films in ethanol or isopropanol aqueous solutions were also measured (Fig. 4). Significant depression on solvent uptakes was observed with the CH/CNT-PSSA nanocomposites. For example, the uptake of CH/CNT-PSSA-1.5 in a 70 wt% ethanol aqueous solution is 25 wt%, which is smaller comparing to the value measured with neat chitosan (43 wt%). The low uptakes of the CH/CNT-PSSA nanocomposites in ethanol aqueous solutions indicate the nanocomposites could be relatively stable in the ethanol aqueous solution. Excepting in water, the uptakes of CH/CNT-PSSA-0.5 were much smaller than the values of CH/CNT-0.5, due to the formation of covalent linkages between chitosan and CNT-PSSA. The relatively high water uptake of CH/CNT-PSSA-0.5 could be understood with the presence of sulfonic acid groups in PSSA chains. More water molecules could associate with the sulfonic acid groups through hydrogen-bonds. In addition to the amounts of water uptakes, the state of absorbed water in the nanocomposites is also of interest, as it plays critical roles in some applications like hydrogel (Li, Xue, & Cheng, 2005; Shin, Kim, Park, Lee, & Kim, 2002) and ion-conducting films (Smitha, Sridhar, & Khan, 2004). The state of water in the nanocomposites films was investigated with a DSC (Higuchi & Iijima, 1985), and the results are collected in Table 1. The "bound water" term refers to the water molecules bound to the nanocomposites with hydrogen bond and the rest could be referred to as "free water". The ratio of bond water to total water

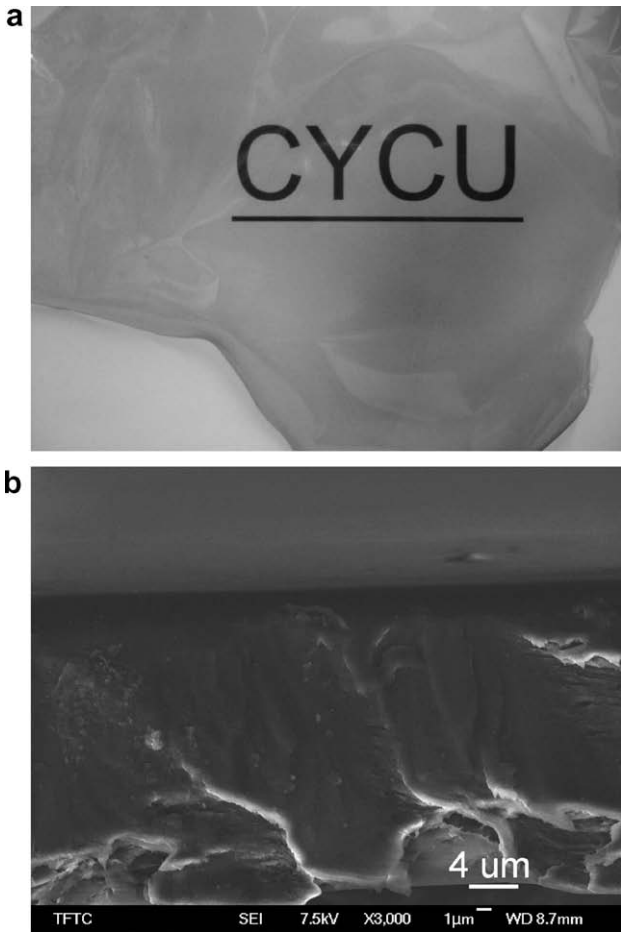

Fig. 2. (a) Photograph of CH/CNT-PSSA-1.5 nanocomposite film exhibiting highly transparent; (b) Cross-sectional scanning electron micrograph (SEM) of CH/CNT-PSSA-1.5 nanocomposite film.

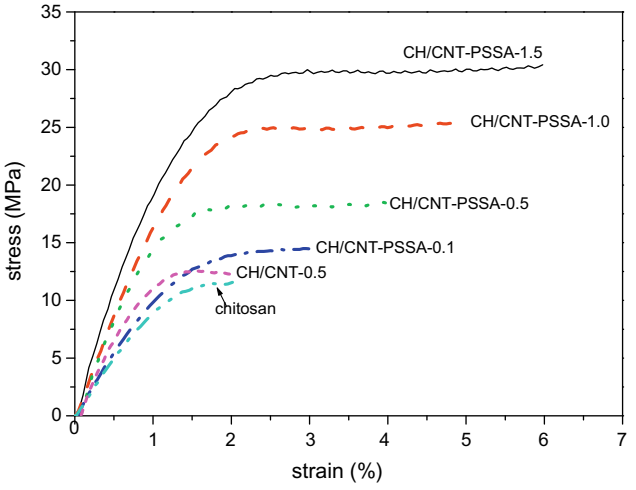

Fig. 3. Stress-strain curves of chitosan and its nanocomposites with carbon nanotubes.

(BWR) of neat chitosan is 22%, indicating some of the absorbed water molecules associating to the amino and hydroxyl groups of chitosan chains with hydrogen bonding. Incorporation of CNT-PSSA to the nanocomposites increases their BWRs. The measured values of BWRs increased with increasing the amounts of CNT-

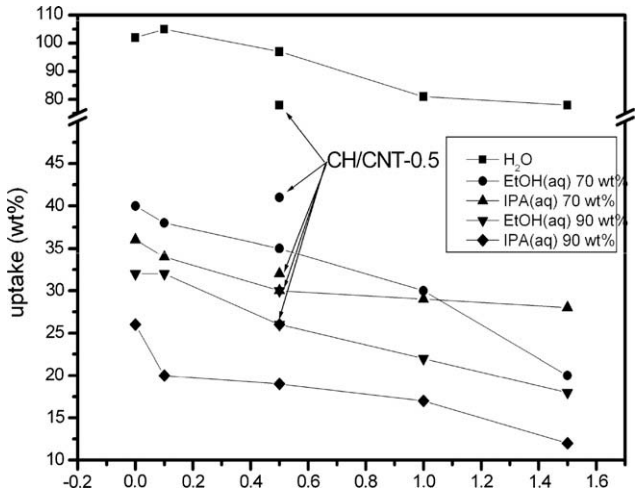

Fig. 4. Water and solvent uptakes of chitosan and its nanocomposites with CNT-PSSA. The data of CH/CNT-0.5 (possessing 0.5 wt% unmodified CNT) is also shown for comparison. EtOH: ethanol, IPA: isopropanol.

PSSA of the nanocomposites, due to the PSSA chains provide additional sites ($-SO_3H$) to bond with water molecules.

CH/CNT-PSSA nanocomposites were utilized as selective membranes for dehydration on a 90 wt% ethanol aqueous solution to probe their application potentials in separation, since chitosan has been widely used as membranes for dehydration separations (Liu, Su, Lee, & Lai, 2005b; Liu, Yu, Lee, & Lai, 2007; Liu et al., 2005a; Shen, Wu, Qiu, & Gao, 2007). Fig. 5 collects the PV performance of the nanocomposite membranes. Since the permeation flux is highly dependent on chitosan molecular weight, membrane thickness, and operation system, the reduced permeation fluxes and separation factors of the nanocomposites are presented. Formation of nanocomposites with CNT-PSSA restricts the molecular chain mobility of chitosan in the ethanol solution with the presence of CNTs and the ionic linkages between chitosan and PSSA chains, so as to decrease their permeation fluxes and increase their selection factors in pervaporation operation. However, the trend is not true for CH/CNT-PSSA-1.5. Addition of too much CNT-PSSA might generate additional pores and voids for ethanol permeation, so as to reduce its separation factor. Similar result has been reported to other composite membranes for pervaporation. It is noteworthy that the pervaporation separation index (PSI) of CH/CNT-PSSA-1.0 is of about 4.67 folds over that of neat chitosan (Table 1), demonstrating the high performance of the CH/CNT-PSSA-1.0 nanocomposite membrane. In addition, CH/CNT-0.5 membrane exhibited a relatively low PSI value, indicating that PSSA modification on CNTs is necessary for the preparation of chitosan/CNT nanocomposites.

Addition of CNT-PSSA to chitosan also increases the electrical conductivities of chitosan from 2.1E-11 to 1.2E-7 S/cm (CH/CNT-PSSA-1.0, data from Fig. 6 at 100 Hz). The increase in electrical conductivity warrants the application potentials of the nanocomposites in electrodes and sensors (Rivas, 2007). Some further work is under studied.

4. Conclusion

PSSA-functionalized CNT was used for preparation of chitosan/CNT nanocomposites, in which ionic linkages between chitosan and CNT-PSSA formed through the reaction between the sulfonic acid groups of PSSA and the amino groups of chitosan. The CH/CNT-PSSA nanocomposites were superior to the neat chitosan polymer in thermal and mechanical properties, water and solvent

Table 1
Properties and pervaporation dehydration performance of the chitosan/CNT nanocomposite membranes on 90 wt% ethanol aqueous solution.

Nanocomposite films	Mechanical properties			Water Contact angle (°)	Bond water ratio[b](wt%)	Pervaporation performance		
	Tensile stress (MPa)	Young's modulus (MPa)	Elongation at break (%)			Reduced flux (RF)[c]	Reduced separation factor (RSF)[d]	Reduced PSI[e]
Neat chitosan	11.6	582	2.0	73	22	1.00	1.00	1.00
CH/CNT-PSSA-0.1	14.5	1373	2.9	72	23	0.74	0.68	0.50
CH/CNT-PSSA-0.5	18.4	2270	3.9	74	34	0.59	1.45	0.85
CH/CNT-PSSA-1.0	25.4	2453	5.0	74	47	0.86	5.43	4.67
CH/CNT-PSSA-1.5	30.4	2815	6.0	86	50	1.02	0.85	0.87
CH/CNT-0.5[a]	12.3	1938	2.0	73	28	0.81	0.56	0.45

[a] Composite made from chitosan and un-modified carbon nanotube for comparison with CH/CNT-PSSA-0.5.
[b] The ratio of bond water over total water absorbed in the nanocomposites.
[c] The permeation flux ratio of nanocomposite over neat chitosan in pervaporation dehydration on a 70 wt% ethanol aqueous solution at 70 °C.
[d] The separation factor ratio of nanocomposite over neat chitosan in pervaporation dehydration on a 70 wt% ethanol aqueous solution at 70 °C.
[e] PSI: pervaporation separation index = permeation flux *separation factor.

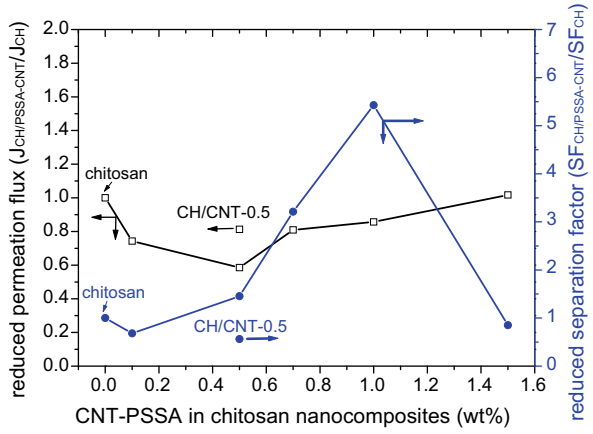

Fig. 5. Pervaporation dehydration performance on a 90 wt% ethanol aqueous solution at 70 °C; reduced permeation flux: flux of nanocomposites/flux of chitosan, reduced separation factor (SF): separation factor of nanocomposites/separation of chitosan.

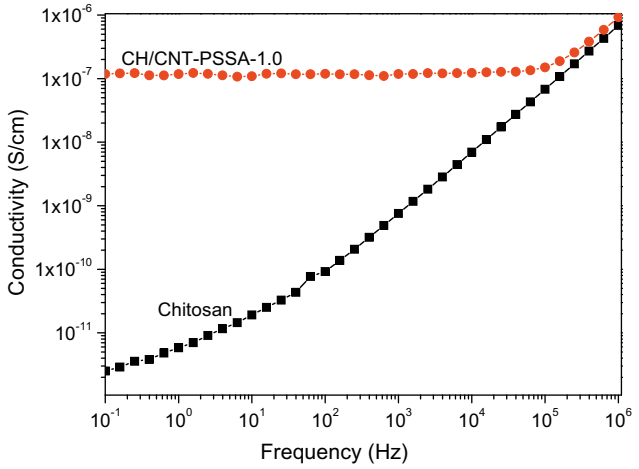

Fig. 6. Electrical conductivities of chitosan and CH/CNT-PSSA-1.0 nanocomposite.

uptakes, bond water ratios, and electrical conductivity. The nanocomposites also exhibited potentials of applications for membrane separation and electrodes.

Acknowledgements

The authors thank the Ministry of Education, Taiwan under the Center-of-Excellence Program on Membrane Science and Technology (2006-2010) for the financial support on this work. The authors also thank Prof. Yu-Chuan Liu (Vanung University, Taiwan) for his kind help on Raman Spectrometry analysis.

References

Darder, M., Colilla, M., & Ruiz-Hitzky, E. (2003). Biopolymer-clay nanocomposites based on chitosan intercalated in montmorillonite. *Chemistry of Materials, 15*, 3774–3780.
Darder, M., López-Blanco, M., Aranda, P., Aznar, A. J., Bravo, J., & Ruiz-Hitzky, E. (2006). Microfibrous chitosan-sepiolite nanocomposites. *Chemistry of Materials, 18*, 1602–1610.
Ding, L., Hao, C., Xue, Y., & Ju, H. (2007). A bio-inspired support of gold nanoparticles-chitosan nanocomposites gel for immobilization and electrochemical study of K562 leukemia cells. *Biomacromolecules, 8*, 1341–1346.
Dong, B., Wang, C., He, B. L., & Li, H. L. (2008). Preparation and tribological properties of poly(methyl methacrylate)/styrene/MWNTs copolymer nanocomposites. *Journal of Applied Polymer Science, 108*, 1675–1679.
Gutierrez, M. C., Jobbagy, M., Ferrer, M. L., & del Monte, F. (2008). Enzymatic synthesis of amorphous calcium phosphate–chitosan nanocomposites and their processing into hierarchical structures. *Chemistry of Materials, 20*, 11–13.
Hao, C., Ding, L., Zhang, X., & Ju, H. (2007). Biocompatible conductive architecture of carbon nanofiber-doped chitosan prepared with controllable electrodeposition for cytosensing. *Analytical Chemistry, 79*, 4442–4447.
Higuchi, A., & Iijima, T. (1985). DSC investigation of the states of water in poly(vinylalcohol-co-itaconic acid) membranes. *Polymer, 26*, 1207–1211.
Hirano, S., Yamaguchi, Y., & Kamiya, M. (2003). Water-soluble *N*-(*n*-fatty acyl)chitosans. *Macromolecular Bioscience, 3*, 629–631.
Hu, Z., Chan, W. L., & Szeto, Y. S. (2008). Nanocomposite of chitosan and silver oxide and its antibacterial property. *Journal of Applied Polymer Science, 108*, 52–56.
Jeon, I. P., Tan, L. S., & Baek, J. B. (2008). Nanocomposites derived from *in situ* grafting of linear and hyperbranched poly(ether-ketone)s containing flexible oxyethylene spacers onto the surface of multiwalled carbon nanotubes. *Journal of Polymer Science Part A: Polymer Chemistry, 46*, 3471–3481.
Jin, H. S., Yoon, K. H., Park, Y. B., & Bang, B. S. (2008). Properties of surface-modified multiwalled carbon nanotube filled poly(ethylene terephthalate) composite films. *Journal of Applied Polymer Science, 107*, 1163–1168.
Kandimalla, V. B., & Ju, H. (2006). Binding of acetylcholinesterase to multiwall carbon nanotube-cross-linked chitosan composite for flow-injection amperometric detection of an organophosphorous insecticide. *Chemistry-A European Journal, 12*, 1074–1080.
Ke, G., Guan, W., Tang, C., Guan, W., Zeng, D., & Deng, F. (2007). Covalent functionalization of multiwalled carbon nanotubes with a low molecular weight chitosan. *Biomacromolecules, 8*, 322–326.
Li, W., Xue, F., & Cheng, R. (2005). States of water in partially swollen poly(vinyl alcohol) hydrogels. *Polymer, 46*, 12026–12031.
Lin, K. F., Hsu, C. Y., Huang, T. S., Chiu, W. Y., Lee, Y. H., & Young, T. H. (2005). A novel method to prepare chitosan/montmorillonite nanocomposites. *Journal of Applied Polymer Science, 98*, 2042–2047.
Liu, Y. L., & Chen, W. H. (2007). Modification of multi-wall carbon nanotubes with initiators and macro-initiators of atom transfer radical polymerization. *Macromolecules, 40*, 8881–8886.
Liu, Y. L., Hsu, C. Y., Su, Y. H., & Lai, J. Y. (2005a). Chitosan-silica complex membranes from sulfuric acid functionalized silica nanoparticles for

pervaporation dehydration of ethanol–water solutions. *Biomacromolecules, 6*, 368–373.

Liu, Y. L., Su, Y. H., Lee, K. R., & Lai, J. Y. (2005b). Crosslinked organic–inorganic hybrid chitosan membranes for pervaporation dehydration of isopropanol/water mixture with a long-term stability. *Journal of Membrane Science, 251*, 233–238.

Liu, Y. L., Yu, C. H., Lee, K. R., & Lai, J. Y. (2007). Chitosan/poly(tetrafluoroethylene) composite membranes using in pervaporation dehydration processes. *Journal of Membrane Science, 287*, 230–236.

Lu, G., Jiang, L., Song, F., Liu, C., & Jiang, L. (2005). Determination of uric acid and norepinephrine by chitosan-multiwall carbon nanotube modified electrode. *Electroanalysis, 17*, 901–905.

Lu, S., Song, X., Cao, D., Chen, Y., & Yao, K. (2004). Preparation of water-soluble chitosan. *Journal of Applied Polymer Science, 91*, 3497–3503.

Podsiadlo, P., Tang, Z., Shim, B. S., & Kotov, N. A. (2007). Counterintuitive effect of molecular strength and role of molecular rigidity on mechanical properties of layer-by-layer assembled nanocomposites. *Nano Letters, 7*, 1224–1231.

Qiu, J. D., Guo, J., Liang, R. P., & Xiong, M. (2007). A nanocomposite chitosan-based on ferrocene-modified silica nanoparticles and carbon nanotubes for biosensor application. *Electroanalysis, 19*, 2335–2341.

Rivas, G. A. (2007). Electrooxidation of DNA at glassy carbon electrodes modified with multiwall carbon nanotubes dispersed in chitosan. *Electroanalysis, 19*, 833–840.

Santos, D. S., Jr., Goulet, P. J. G., Pieczonka, N. P. W., Oliveira, O. N., Jr., & &Aroca, R. F. (2004). Gold nanoparticle embedded, self-sustained chitosan films as substrates for surface-enhanced Raman scattering. *Langmuir, 20*, 10273–10277.

Sashiwa, H., Kawasaki, N., Nakayama, A., Muraki, E., Yamamoto, N., & Aiba, S.-I. (2002). Chemical modification of chitosan. *Biomacromolecules, 3*, 1126–1128.

Sashiwa, H., Yamamori, N., Ichinose, Y., Sunamoto, J., & Aiba, S. (2003). Chemical modification of chitosan. *Macromolecular Bioscience, 3*, 231–233.

Shen, J. N., Wu, L. G., Qiu, J. H., & Gao, C. J. (2007). Pervaporation separation of water/isopropanol mixtures through crosslinked carboxymethyl chitosan/polysulfone hollow-fiber composite membranes. *Journal of Applied Polymer Science, 103*, 1959–1965.

Shin, M. S., Kim, S. J., Park, S. J., Lee, Y. H., & Kim, S. I. (2002). Synthesis and characteristics of the interpenetrating polymer network hydrogel composed of chitosan and polyallylamine. *Journal of Applied Polymer Science, 86*, 498–503.

Smitha, B., Sridhar, S., & Khan, A. A. (2004). Polyelectrolyte complexes of chitosan and poly(acrylic acid) as proton exchange membranes for fuel cells. *Macromolecules, 37*, 2233–2239.

Wang, S., Chen, L., & Tong, Y. (2006). Structure-property relationship in chitosan-based biopolymer/montmorillonite nanocomposites. *Journal of Polymer Science Part A: Polymer Chemistry, 44*, 686–696.

Wang, J., Dai, J., & Yarlagadda, T. (2005a). Carbon nanotube-conducting-polymer composite nanowires. *Langmuir, 21*, 9–12.

Wang, X., Du, Y., Yang, J., Tang, Y., & Luo, J. (2008). Preparation, characterization, and antimicrobial activity of quaternized chitosan/organic montmorillonite nanocomposites. *Journal of Biomedical Materials Research, 84A*, 384–390.

Wang, S. F., Shen, L., Zhang, W. D., & Tong, Y. J. (2005b). Preparation and mechanical properties of chitosan/carbon nanotubes composites. *Biomacromolecules, 6*, 3067–3072.

Wang, L., & Wang, A. (2007). Removal of congo red from aqueous solution using a chitosan/organo- montmorillonite nanocomposites. *Journal of Chemical Technology and Biotechnology, 82*, 711–720.

Xu, Z., Gao, N., Chen, H., & Dong, S. (2005). Biopolymer and carbon nanotubes interface prepared by self-assembly for studying the electrochemistry of microperoxidase-11. *Langmuir, 21*, 10808–10813.

Xu, Y., Ren, X., & Hanna, M. A. (2006). Chitosan/clay nanocomposite film preparation and characterization. *Journal of Applied Polymer Science, 99*, 1684–1691.

Xu, D.-H., Wang, Z.-G., & Douglas, J. F. (2008). Influence of carbon nanotube aspect ratio on normal stress differences in isotactic polypropylene nanocomposite melts. *Macromolecules, 41*, 815–825.

Zhang, J., Wang, L., & Wang, A. (2007). Preparation and properties of chitosan-*g*-poly(acrylic acid)/montmorillonite superabsorbent nanocomposite via in situ intercalative polymerization. *Industrial and Engineering Chemical Research, 46*, 2497–2502.